Journal of Geothermal Research and Volcanology (2026) 01-08

Contents lists available at FoundAE

Journal of Geothermal Research and Volcanology

Journal homepage: https://ejournal.foundae.com/index.php/jograv/index

Gravity-based 3D imaging of subsurface heat source and structural controls in the Pemali non-volcanic geothermal, Bangka Island, Indonesia

Putriani[a,1], Rahmat Nawi Siregar[b,*,1], Glenaldo Achmad Zhafran Evito[c]

[a] Department of Physics, Institut Teknologi Sumatera, Way Huwi, Jati Agung, South Lampung, Lampung 35365, Indonesia
[b] Department of Physics, Institut Teknologi Sumatera, Way Huwi, Jati Agung, South Lampung, Lampung 35365, Indonesia
[c] School of Integrative and Global Majors, University of Tsukuba, Tsukuba, Ibaraki 305-0006, Japan

ARTICLE INFO

Keywords:
Non-volcanic geothermal system
Satellite gravity data
3D gravity inversion
Granite intrusion
Structural control

ABSTRACT

The Southeast Asian Tin Belt is characterized by extensive granitoid intrusions that may act as long-lived heat sources for non-volcanic geothermal systems. On Bangka Island, Indonesia, hot spring manifestations in the Pemali area (North Bangka Regency) indicate active geothermal circulation unrelated to recent volcanism. This study aims to characterize the subsurface structure and identify the principal structural controls governing the Pemali geothermal system, with particular emphasis on delineating buried granite intrusions and associated fault zones that may facilitate heat transfer and fluid migration. Secondary satellite-derived gravity data (TOPEX) were analyzed through regional–residual separation and three-dimensional inversion modeling to reconstruct subsurface density distribution. The regional gravity anomaly ranges from 21.7 to 38.1 mGal and reflects deep-seated high-density basement or intrusive bodies consistent with granitoid emplacement. Residual anomalies vary from −2.4 to 1.5 mGal, indicating shallow lateral density contrasts. Prominent low residual gravity zones are interpreted as fractured and altered rocks with reduced density, likely associated with geothermal fluid pathways and structural discontinuities. These anomalies spatially correlate with surface thermal manifestations, suggesting structurally controlled geothermal circulation. The results support a conceptual model in which heat is conducted from subsurface granite bodies into overlying Tanjung Genting Formation rocks, while faults and fractures enhance permeability and fluid flow. This study demonstrates that integrated gravity inversion provides an effective reconnaissance tool for identifying heat sources and structural controls in non-volcanic geothermal settings, offering a geophysical basis for further detailed exploration in the Pemali geothermal prospect.

1. Introduction

Global demand for sustainable and low-carbon energy resources has intensified interest in geothermal systems, particularly those that are not directly associated with active volcanism. While volcanic geothermal systems are widely studied due to their high enthalpy and surface manifestations, non-volcanic geothermal systems hosted by intrusive bodies represent an underexplored but potentially significant energy resource [1, 2]. In many tectonically stable or post-magmatic regions, granitoid intrusions can act as long-lived heat sources capable of sustaining geothermal circulation through conductive heat transfer and structurally controlled fluid flow. Understanding the subsurface configuration of such systems is therefore essential for reducing exploration risk and improving resource assessment.

The Southeast Asian Tin Belt, extending from Myanmar through Thailand and Malaysia to Indonesia, is characterized by widespread Mesozoic granitoid intrusions associated with tin mineralization [3–5]. Bangka Island, located in western Indonesia, forms part of this metallogenic province and is dominated by granitic and granitoid rocks emplaced during regional tectono-magmatic events [6, 7]. These intrusive bodies are known to possess elevated radiogenic heat production due to the enrichment of uranium, thorium, and potassium-bearing minerals, which may contribute to long-term subsurface heat anomalies (Fig. 1). Although the region lacks active volcanism, several thermal manifestations, including hot springs, have been reported, suggesting the existence of non-volcanic geothermal systems potentially related to buried granite intrusions [8–10].

* Corresponding author.
E-mail address: rahmat.siregar@fi.itera.ac.id (R. N. Siregar).
[1] These authors contributed equally to this work.

https://doi.org/10.58524/jograv.v1i1.104
Received 1 January 2026; Received in revised form 1 February 2026; Accepted 10 February 2026
Available online 1 March 2026
3163-3471/Published by FoundAE (Foundation of Advanced Education).

One such manifestation occurs in the Pemali area, North Bangka Regency, where hot springs indicate ongoing geothermal circulation. Unlike volcanic geothermal systems, where magma chambers and recent eruptive activity provide clear heat sources, the thermal regime in Pemali is likely controlled by conductive heat transfer from intrusive granite bodies and enhanced by structural permeability [3, 11]. In this context, faults and fracture systems play a crucial role by facilitating the migration of heated fluids from depth toward the surface. Therefore, identifying subsurface intrusive bodies and mapping structural discontinuities are key steps in evaluating the geothermal potential of the area [12, 13].

Geophysical methods offer a cost-effective approach for regional reconnaissance in geothermal exploration, particularly in areas where drilling data are limited [6, 14, 15]. Among these methods, gravity surveying is widely applied to delineate subsurface density contrasts associated with lithological variations, intrusive bodies, and structural features [4, 16]. Granite intrusions, depending on their composition and alteration state, may exhibit density contrasts relative to surrounding sedimentary or metamorphic rocks. In addition, fault zones often appear as localized density anomalies due to fracturing, hydrothermal alteration, and fluid saturation. Consequently, gravity anomaly analysis can provide valuable constraints on subsurface geometry and structural architecture [17, 18].

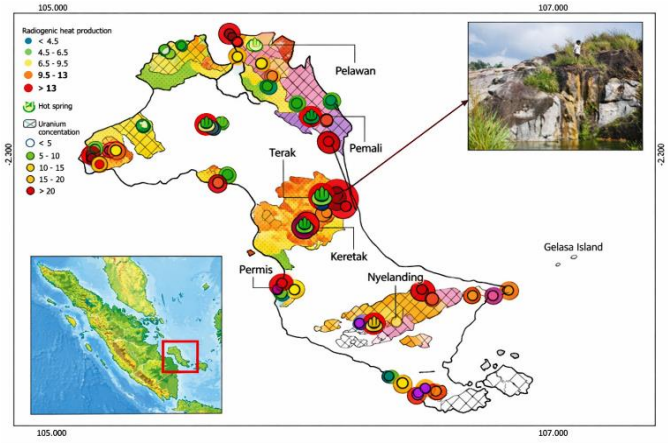

Fig. 1. Radiogenic heat production map of Bangka Island based on uranium concentration.

Recent advances in satellite-derived gravity datasets, such as TOPEX/Poseidon, have enabled large-scale gravity investigations in regions where ground-based measurements are sparse or logistically challenging. Although satellite gravity data generally have lower spatial resolution compared to detailed terrestrial surveys, they are particularly useful for regional structural mapping and preliminary geothermal prospect evaluation [3, 6, 16]. By separating regional and residual gravity components, it is possible to distinguish deep-seated density structures from shallow heterogeneities. Furthermore, three-dimensional (3D) inversion modeling allows reconstruction of subsurface density distributions that are consistent with observed gravity anomalies, thereby providing a more quantitative basis for geological interpretation [19–21].

In geothermal exploration, integrated gravity inversion has been successfully applied to identify heat sources, intrusive bodies, caldera structures, and fault-controlled permeability pathways. For non-volcanic geothermal systems, gravity methods are especially relevant because the primary heat source is often associated with crystalline basement or granitoid intrusions that may not produce strong surface expressions. In such settings, density variations related to intrusive emplacement, structural segmentation, and alteration zones can be used to construct a conceptual geothermal model.

Despite the geological significance of Bangka Island within the Southeast Asian Tin Belt, geophysical investigations targeting geothermal potential remain limited. Previous studies have focused primarily on mineral exploration, particularly tin deposits, while the geothermal implications of granitoid intrusions have received comparatively little attention. In the Pemali area, the presence of hot spring manifestations indicates that subsurface heat and fluid circulation are active, yet the geometry of the underlying heat source and the structural framework controlling fluid migration remain poorly constrained. A regional-scale gravity analysis can therefore provide fundamental insights into the subsurface configuration and help establish a preliminary geothermal exploration model [3, 6, 16].

This study aims to characterize the subsurface structure of the Pemali geothermal prospect using satellite-derived gravity data (TOPEX) combined with regional–residual anomaly separation and 3D inversion modeling. Specifically, the objectives are: (1) to delineate deep-seated density anomalies that may represent granite intrusions acting as heat sources; (2) to identify shallow structural discontinuities potentially associated with fault-controlled permeability; and (3) to develop a conceptual geothermal model that integrates gravity-derived subsurface structures with surface thermal manifestations [6, 14, 15].

The methodological approach involves processing gravity anomaly data to separate regional trends from residual components, followed by quantitative 3D inversion to reconstruct subsurface density contrasts. Regional anomalies are interpreted to reflect deep crustal or basement-scale structures, whereas residual anomalies are analyzed to highlight shallow density variations linked to geothermal features. Low-density residual zones are evaluated in relation to possible fracture systems and hydrothermal alteration, while high-density anomalies are assessed as potential intrusive bodies [19–21].

By integrating gravity anomaly interpretation with geological context, this study seeks to provide a reconnaissance-level assessment of the Pemali geothermal system. The results are expected to contribute to a better understanding of granite-hosted, non-volcanic geothermal systems within the Southeast Asian Tin Belt and to demonstrate the applicability of satellite gravity data in early-stage geothermal exploration. Ultimately, this research provides a geophysical foundation for more detailed investigations, including ground-based geophysical surveys, geochemical analyses, and exploratory drilling, to further evaluate the geothermal potential of the Pemali area.

2. Conceptual geological setting

2.1. Regional Tectonic Framework

Bangka Island is part of the western Indonesian region and belongs to the Southeast Asian Tin Belt, a major metallogenic province extending from Myanmar through Thailand and Malaysia to Indonesia. The tectonic evolution of this belt is closely related to Mesozoic magmatic activity associated with subduction and subsequent post-collisional processes along the Eurasian margin. During the Late Triassic to Cretaceous, large volumes of granitoid intrusions were emplaced throughout the region, forming extensive batholithic complexes that are now widely exposed in Peninsular Malaysia and the Indonesian islands of Bangka and Belitung.

The granitoids of Bangka Island are generally classified as I-type to S-type granites, commonly associated with tin mineralization and enriched in radiogenic elements such as uranium (U), thorium (Th), and potassium (K). These elements contribute to internal heat production through radioactive decay, allowing the intrusive bodies to retain elevated thermal conditions over geological timescales. Although the region is not characterized by recent volcanism, the presence of such granitoid bodies suggests the potential for non-volcanic geothermal systems sustained by long-term conductive heat transfer.

Structurally, Bangka Island is influenced by regional fault

systems related to past tectonic deformation phases. These structures include NW–SE and NE–SW trending faults, which are interpreted to reflect compressional and extensional regimes associated with plate interactions between the Sundaland block and adjacent tectonic domains. Such fault systems not only control mineralization patterns but may also provide structural pathways for geothermal fluid circulation.

2.2. *Lithological characteristics of Bangka island*

The lithology of Bangka Island is dominated by intrusive granitoid rocks and sedimentary formations. The granitic intrusions are typically medium- to coarse-grained and locally weathered, forming extensive plutonic bodies across the island. These granitoids intrude older sedimentary sequences and are often associated with contact metamorphism and hydrothermal alteration.

In the northern part of Bangka, including the Pemali area, granitoid rocks are overlain or juxtaposed with sedimentary formations such as the Tanjung Genting Formation. This formation generally consists of sandstones, siltstones, and claystones that may exhibit varying degrees of compaction and alteration. The density contrast between crystalline granite and overlying sedimentary rocks provides a favorable condition for gravity-based subsurface investigation.

From a geothermal perspective, the granite bodies serve as the primary heat source, while the overlying sedimentary and fractured zones may act as reservoirs or cap rocks, depending on permeability distribution. The degree of fracturing and hydrothermal alteration significantly influences the effective porosity and permeability of these units, thereby controlling fluid migration and heat transport.

2.3. *Structural control and fluid circulation*

In non-volcanic geothermal systems, structural features play a fundamental role in governing subsurface fluid circulation. Unlike volcanic systems where magmatic heat is typically shallow and intense, non-volcanic systems rely on deep-seated heat sources and permeable pathways to transfer thermal energy toward the surface. Faults, fractures, and shear zones enhance permeability and allow meteoric water to infiltrate, circulate at depth, and return as thermal manifestations such as hot springs.

In the Pemali area, surface hot spring occurrences suggest active hydrothermal circulation. The structural framework likely consists of fault-controlled conduits that connect deeper heated zones within granite bodies to shallow sedimentary layers. Fracturing associated with regional tectonics may create localized zones of reduced density due to increased porosity and alteration, which can be detected as residual gravity anomalies.

The interplay between intrusive emplacement and tectonic deformation is particularly important. Granite intrusions may generate thermal metamorphism and induce stress redistribution, potentially reactivating pre-existing faults. These reactivated faults can subsequently serve as preferential pathways for geothermal fluids. Therefore, mapping structural discontinuities is crucial for understanding the geometry and sustainability of the geothermal system.

2.4. *Heat source mechanism in granite-hosted systems*

Granite-hosted geothermal systems differ fundamentally from magmatic volcanic systems. The primary heat source is not a young magma chamber but rather residual and radiogenic heat within crystalline basement rocks. Radiogenic heat production in granites is largely controlled by the concentration of U, Th, and K-bearing minerals. Over geological time, this internal heat production may sustain elevated geothermal gradients, especially in regions with relatively thick crust and limited convective cooling.

Heat transfer in such systems occurs predominantly through conduction from the granite body to surrounding rocks. However, once permeability pathways are established through faulting and fracturing, convection may significantly enhance heat extraction and surface expression. The interaction between conductive heat flow and convective fluid movement defines the geothermal system's efficiency.

In the context of Pemali, the conceptual model assumes that subsurface granite intrusions provide a long-term heat reservoir. The overlying Tanjung Genting Formation may act as a host for circulating fluids, while structural discontinuities facilitate vertical and lateral flow. Zones of hydrothermal alteration may further modify physical properties such as density, magnetic susceptibility, and electrical resistivity, making them detectable through geophysical methods.

3. Method

3.1. *Study area and data source*

The study was conducted in the Pemali geothermal prospect, located in North Bangka Regency, Bangka Island, Indonesia. Geographically, the study area lies between 1°45′–2°08′ S and 105°47′–106°45′ E. The region is characterized by granitic intrusions associated with the Southeast Asian Tin Belt and surface hot spring manifestations indicative of geothermal activity. Data processing and modeling were carried out between October 2021 and July 2022 at the Geophysics Laboratory, Physics Study Program, Institut Teknologi Sumatera, Indonesia (Fig. 2).

This study utilizes secondary satellite-derived gravity data obtained from the TOPEX database (https://topex.ucsd.edu

), accessed on November 30, 2021. The dataset consists of gridded Free Air Anomaly (FAA) values in ASCII-XYZ format, including latitude, longitude, elevation, and gravity anomaly values. Topographic data were obtained from the Shuttle Radar Topography Mission (SRTM) dataset provided by the United States Geological Survey (USGS). Regional geological maps were used to constrain lithological interpretation and density parameter selection.

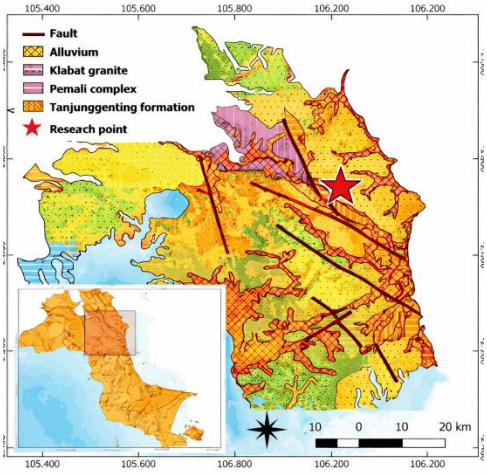

Fig. 2. Geothermal observation point of gravity data in Pemali, Bangka Island, Indonesia with geology information.

3.2. *Gravity data processing*

Gravity data processing was conducted in two main stages: (1) gravity correction and Complete Bouguer Anomaly (CBA) calculation, and (2) anomaly separation and subsurface modeling. [14, 22, 23]. The raw dataset consisted of Free Air Anomaly (FAA) values. To obtain the Complete Bouguer Anomaly (CBA), the following corrections were applied:

- Free Air Correction (FAC)
- Bouguer Slab Correction
- Terrain Correction (TC)

The Bouguer correction accounts for the gravitational effect of the rock mass between the observation point and the reference datum. Terrain correction compensates for topographic variations surrounding measurement points and was computed using SRTM elevation data.

An optimal Bouguer density was estimated through correlation analysis between elevation and Bouguer anomaly values using density variations ranging from 1.7 to 2.3 g/cm³. The density value that minimized correlation between gravity anomaly and elevation was selected as the representative surface density. The Complete Bouguer Anomaly (CBA) was calculated as:

$$CBA = FAA - Bouguer\ Correction + Terrain\ Correction \quad \ldots (1)$$

The corrected dataset was subsequently converted into UTM Zone 48S coordinates for spatial analysis.

3.3. Spectral analysis and regional–residual separation

To estimate source depth and separate regional and residual components, spectral analysis was performed using Fourier Transform techniques implemented in Oasis Montaj. The logarithmic power spectrum was analyzed by plotting log amplitude against wavenumber. The slope of the spectrum was used to estimate the average depth of anomaly sources. A cut-off wavenumber was determined based on the transition between deep (regional) and shallow (residual) sources, supported by the coefficient of determination (R^2) as a control parameter. Regional and residual anomalies were separated using frequency-domain filtering:

- Low-pass filter → isolates deep regional anomalies
- Band-pass filter → highlights shallow residual anomalies

Residual anomalies are interpreted to represent shallow density contrasts related to structural features and geothermal circulation pathways.

3.4. Two and three-dimensional forward modeling

Two-dimensional forward modeling was conducted along selected profiles crossing significant gravity anomalies. The objective was to estimate subsurface geometry and density distribution consistent with observed gravity responses. Modeling was performed using Oasis Montaj, integrating geological constraints. A trial-and-error forward modeling approach was applied until the misfit between observed and calculated anomalies was minimized (error <5%). The minimum and maximum density values obtained from 2D modeling were used as constraints for subsequent 3D inversion modeling.

Three-dimensional gravity modeling was performed using Grablox 1.6e, with visualization in Bloxer 1.6e. The workflow consisted of:

1. Initial Forward Modeling
   A block model representing the study area was constructed based on gridded Complete Bouguer Anomaly data. Major and minor blocks were defined according to spatial resolution and area extent.
2. Density Parameter Assignment
   Density values derived from 2D modeling were assigned as initial constraints.
3. Inverse Modeling
   An iterative inversion procedure was applied to adjust density distribution and geometry to minimize misfit between observed and calculated gravity anomalies. Optimization stages included:
   - Base model adjustment
   - Density optimization
   - Occam density smoothing
   - Elevation adjustment
   - Occam height smoothing

The inversion process aimed to reduce residual error and obtain a geologically reasonable subsurface density model.

3.5. Data interpretation

Interpretation was conducted qualitatively and quantitatively. For the qualitative interpretation, gravity anomaly maps (Complete Bouguer, regional, and residual) were analyzed to identify patterns associated with density contrasts. High gravity anomalies were interpreted as potential granitoid intrusions or basement highs, whereas low residual anomalies were interpreted as fractured or altered zones possibly associated with geothermal fluid pathways.

While quantitative interpretation, the cross-sectional models from 2D forward modeling and volumetric density distributions from 3D inversion were integrated with geological maps. Density contrasts were correlated with lithological units and structural features, particularly fault systems that may act as geothermal conduits.

- The final interpretation focuses on identifying:
- Potential granite heat sources
- Structural controls (faults/fractures)
- Zones of reduced density indicative of hydrothermal alteration

4. Results and discussion

4.1. Complete bouguer anomaly (CBA) map

The Complete Bouguer Anomaly (CBA) map is derived from gravity data processing and represents the spatial distribution pattern of subsurface rock density. In this study, the CBA map is presented using the UTM coordinate system, Zone 48 in the Southern Hemisphere, as shown in the corresponding figure. The color range on the map indicates variations in gravity anomaly values, which reflect differences in subsurface rock density within the study area. This variation suggests that the subsurface lithology is heterogeneous both laterally and vertically, resulting in different CBA values across the region.

The obtained Complete Bouguer anomaly values range from 21.3 mGal to 38.4 mGal, and all values are positive. The differences in the color scale (in mGal) indicate variations in anomaly intensity across the study area. Low gravity anomalies occur within the range of 21.3–29.7 mGal and are predominantly distributed in the northwestern part of the study area. In contrast, high gravity anomalies range from 29.7–38.4 mGal and are mainly distributed in the northern and western parts of the study area.

The presence of low gravity anomalies on the CBA map can be interpreted as zones with lower subsurface density compared to surrounding areas. Such conditions may indicate geothermal manifestations, such as altered rocks, fracture zones filled with fluids, or the accumulation of hot water beneath the surface.

However, the CBA map represents the combined effect of both deep and shallow sources. Therefore, to better understand the subsurface structure and to distinguish between deep regional effects and shallow local anomalies associated with geothermal features, it is necessary to separate the anomaly into regional and residual components. This separation is carried out using spectral analysis [24].

4.2. Spectral analysis

Spectral analysis was applied to estimate the depth of gravity anomaly sources within the study area. This method also serves as a reference for separating regional and residual anomaly components. Regional anomalies generally originate from deeper sources and are characterized by long wavelengths (low frequency), whereas residual anomalies are associated with shallower sources and exhibit short wavelengths (high frequency) [20, 21, 25].

The spectral analysis graph in this study presents the relationship between the logarithm of amplitude (ln A) and the wavenumber (k). Based on this graph, cut-off wavenumbers can be estimated to determine the filter window width. Furthermore, this curve is used to estimate the depth of regional, residual, and noise anomaly sources.

The Fig. 3 shows the spectral analysis curve separating regional, residual, and noise components. The Fourier Transform produces a curve representing the relationship between wavenumber (k) and the logarithm of amplitude (ln A). The curve displays three linear segments, each representing discontinuity surfaces at different depths. These segments are identified based on their coefficient of determination (R^2), which indicates the degree of correlation between the independent variable

(wavenumber) and the dependent variable (logarithm of amplitude).

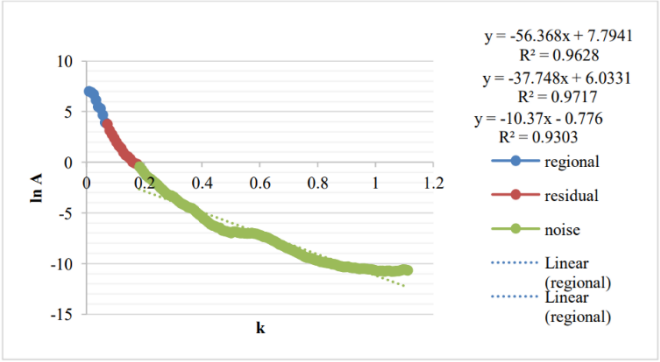

Fig. 3. Curve of spectral analysis of regional anomalies, residuals, and noise separation.

From the curve, cut-off wavenumbers are obtained to distinguish the regional, residual, and noise zones. The boundary between the regional and residual zones is defined by a wavenumber of k = 0.0634921, while the boundary between the residual and noise zones is defined by k = 0.174603. These cut-off wavenumbers are used to estimate the depth of anomaly sources through spectral analysis, based on the filter window width derived from the curve.

The depth estimation results are presented in Fig. 4, which shows the spectral analysis curve and the calculated depth values obtained from the Fourier Transform using Oasis Montaj software. Based on the analysis, the regional anomaly is estimated to occur at a depth of approximately 4.56 km, while the residual anomaly is estimated to occur within a depth range of approximately 1.68 km to 4.56 km.

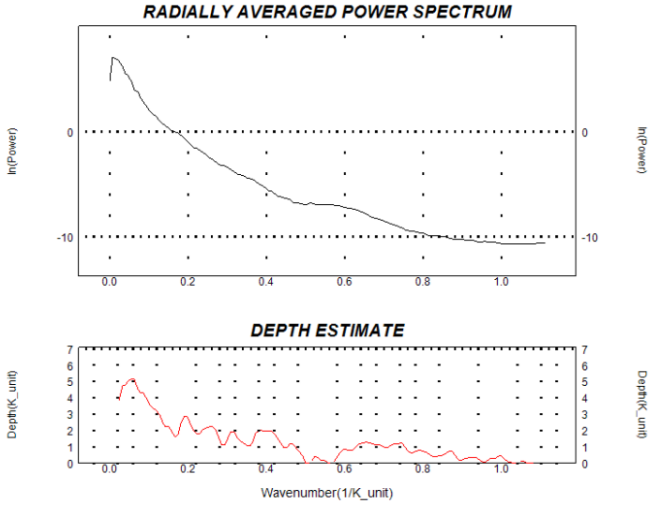

Fig. 4. Spectrum analysis curve and depth estimation.

The residual anomalies, which correspond to shallower depths, are considered more relevant to the interpretation of local geological structures and potential geothermal systems. Meanwhile, the regional anomaly reflects deeper geological structures that control the broader tectonic framework of the study area.

4.3. Separation of regional and residual anomalies

The separation of regional and residual anomalies was carried out based on the spectral analysis of the relationship between ln A and the wavenumber (k). After determining the cut-off wavenumbers, the regional, residual, and noise components were separated through filtering of the complete bouguer anomaly (CBA) contour map. The filtering process produced regional and residual anomaly maps that were reduced from noise components.

The separation was performed using the Butterworth filter and Bandpass filter in Oasis Montaj software. The Butterworth filter was applied to separate the regional component (characterized by low frequency and long wavelength) from the residual component. Meanwhile, the Bandpass filter was used to reduce high-frequency noise within the residual zone. This separation aims to distinguish between deep-seated and shallow anomaly sources. Fig. 5 presents the regional anomaly map, while Fig. 6 shows the residual anomaly map.

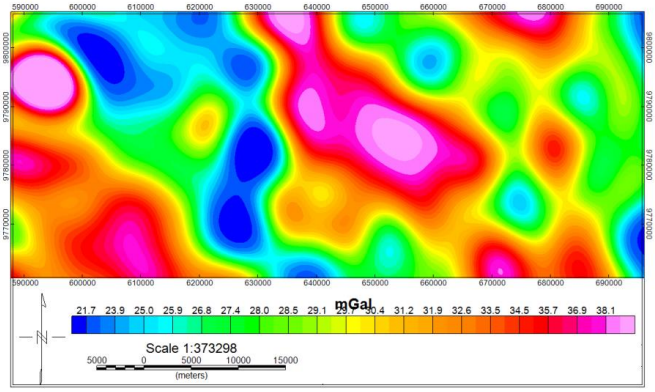

Fig. 5. Regional gravity anomaly map.

The regional anomaly reflects deeper causative sources, whereas the residual anomaly is associated with shallower subsurface sources. The results show clear differences in anomaly magnitude and contour patterns between the regional and residual components. The regional anomaly exhibits positive values ranging from 21.7 mGal to 38.1 mGal. In contrast, the residual anomaly displays smaller amplitude variations, ranging from −2.4 mGal to 1.5 mGal, including both negative and positive values. This indicates that the residual anomaly originates from shallower sources with more variable density contrasts compared to the regional component [16, 26, 27].

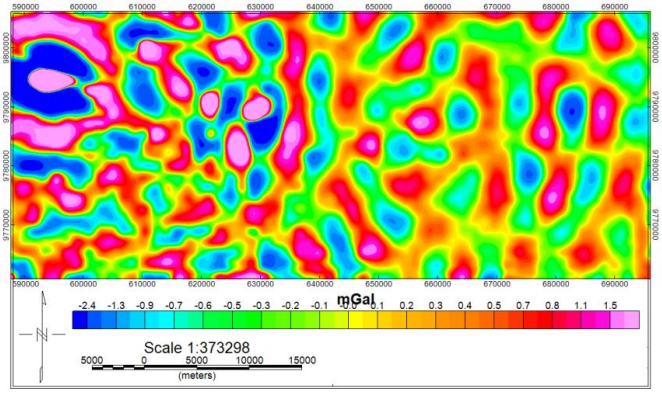

Fig. 6. Residual gravity anomaly map.

The residual (local) anomaly was obtained by subtracting the regional component from the Complete Bouguer Anomaly map. Based on the residual values, low anomalies range from −2.4 mGal to −0.1 mGal, while high anomalies range from 0.0 mGal to 1.5 mGal. Topographic variations may also influence measured gravity values. Generally, higher elevations tend to produce lower gravity values, while lower elevations correspond to relatively higher gravity values. Therefore, topographic effects must be considered in interpreting the residual gravity anomaly patterns.

4.4. 2D gravity anomaly modeling

Two-dimensional (2D) gravity modeling of the study area was

carried out using the complete bouguer anomaly (CBA) map, supported by geological data and regional stratigraphic information. The modeling profile was constructed along the A–A' cross-section, as shown in the figure below. The profile extends from the southwest to the northeast across the Pemali geothermal area, North Bangka Regency. Fig. 7 shows the location of the A–A' profile on the Complete Bouguer Anomaly map.

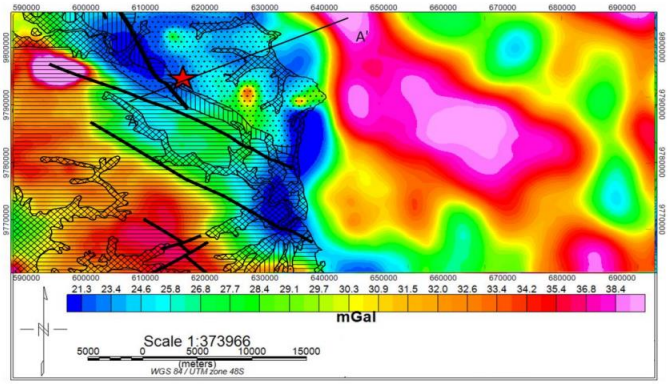

Fig. 7. The A-A' line on the complete bouguer anomaly map.

The 2D modeling results consist of two main outputs: (1) the forward modeling curve and (2) the subsurface density model. In the forward modeling curve, the observed gravity data are represented by black dots, while the calculated gravity response from the model is shown by the black line. The red line represents the error (misfit) between the observed and calculated values. The modeling produced an error value of 3.478%, indicating a relatively good agreement between the observed data and the calculated response. Along the A–A' profile, the Bouguer anomaly values range from approximately 20 mGal to 40 mGal. Starting from point A, the profile crosses a positive Bouguer anomaly zone with an initial anomaly value of approximately 28.4 mGal, then increases to a maximum value of 38.4 mGal at a distance of about 39 km from the starting point. Fig. 8 presents the forward modeling curve and the resulting 2D gravity model of the Pemali geothermal area.

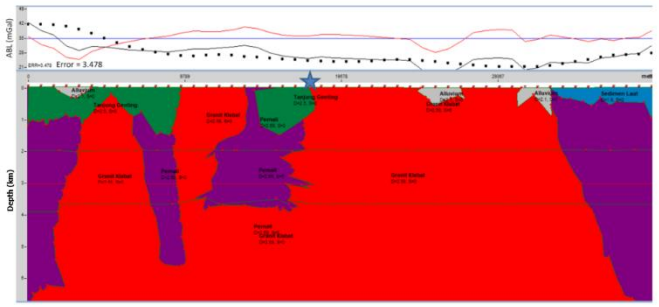

Fig. 8. Forward modelling curve and 2D modelling in the Pemali geothermal area.

Based on the stratigraphic data of North Bangka, the A–A' profile intersects four main geological units. The Pemali Metamorphic Complex (CPp) forms the basement of the Bangka region, consisting of phyllite, quartzite, and schist, with an assumed density of 2.69 g/cm³. The second unit is the Klabat Granite, composed of biotite granite, gneissic granite, and granodiorite, with a density of 2.58 g/cm³. The next unit is the Tanjung Genting Formation, dominated by sandstone and claystone, with a density of 2.50 g/cm³. The uppermost unit consists of alluvial deposits, composed of boulders, cobbles, gravel, sand, clay, and peat, with a density of 2.10 g/cm³. Two faults were interpreted along the A–A' profile. These faults form a graben structure, characterized by a down-dropped central block resulting from tectonic processes. The graben structure is interpreted to play an important role in the formation of a geothermal reservoir, as it provides space for meteoric water to accumulate before being heated by the underlying granite intrusion. The hot spring manifestation is interpreted to occur within the Tanjung Genting Formation, which acts as a heat-conducting unit after interacting with the granite body.

As a result, the thermal manifestation in the Pemali geothermal area is not associated with volcanic activity. Therefore, the temperature of the hot spring is relatively low compared to volcanic geothermal systems, ranging approximately between 40–60°C.

4.5. 3D gravity anomaly modeling

In the 3D modeling process, two main stages were carried out: forward modeling and inversion modeling. During the forward modeling stage, an initial model was constructed to represent the spatial extent of the study area. The study area covers 107.5569871 km in the x-direction and 44.273711 km in the y-direction. The area was then discretized into 20 minor blocks in each horizontal direction, resulting in a total of 400 minor blocks per layer.

In the vertical direction (z-axis), the model depth was defined up to 6.8 km and divided into 8 minor blocks, resulting in a total of 3,200 minor blocks for the entire 3D model. The density range assigned in the initial model varies from 1 g/cm³ to 3 g/cm³. This density range was determined based on the results of the previous 2D gravity modeling conducted using Oasis Montaj software. After constructing the initial model, the inversion process was performed by matching the modeled gravity response with the observed field data using a mathematical approach. The objective of this inversion stage is to estimate the unknown subsurface physical parameters and obtain a model that best fits the observed gravity data [16].

During the inversion modeling process, the Complete Bouguer Anomaly (CBA) data were used as the primary input to generate the subsurface model. After the CBA data were incorporated, the inversion procedure was carried out through five optimization stages to reduce the error (misfit) between the calculated model response and the observed field data. These stages include: base optimization, density optimization, Occam density optimization (Occam d), height optimization, and Occam height optimization (Occam h).

The Occam height optimization (Occam h) represents the final stage of the entire inversion process. This step aims to obtain the best-fit Bouguer anomaly pattern by minimizing discrepancies between the modeled and observed gravity data while maintaining model smoothness and stability. The final optimized model was subsequently used for further interpretation, as it represents the integrated result of all optimization stages. After completing the optimization process, the inversion modeling results were imported into Grablox 1.6e software to visualize the subsurface structure in three dimensions. The 3D subsurface model of the study area, based on the Complete Bouguer gravity anomaly data, is presented in Fig. 9. The 3D model consists of eight layers, extending to a maximum depth of approximately 6.83 km.

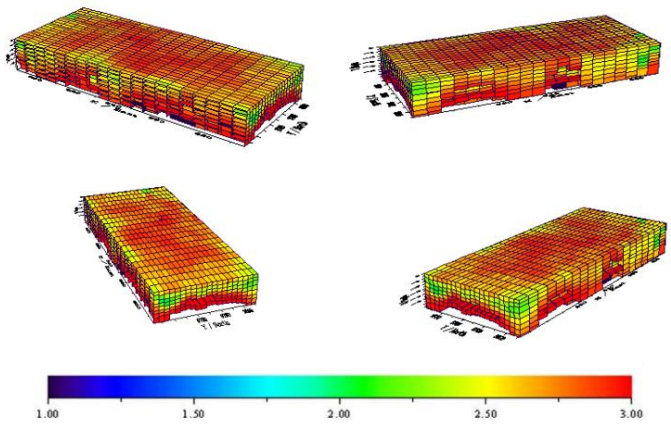

Fig. 9. 3D subsurface model of the Pemali geothermal area.

According to the visualization results, Layer 5 is located at a depth range of approximately 2.54 km to 3.41 km. This layer exhibits density values ranging from 1.70 g/cm³ to 2.75 g/cm³, with an average density of approximately 2.49 g/cm³. The average density suggests that this layer is dominated by medium- to high-density rocks, which may correspond to compact sedimentary formations or intrusive igneous rocks at that depth.

The advanced interpretation results are presented in the Fig. 8, that the 2D model along profile A–A', which indicates the presence of faults associated with a graben structure expressed as a valley. This structure is interpreted to control geothermal manifestations by forming a geothermal reservoir. Meteoric water infiltrates from the surface, accumulates within the reservoir zone, and is subsequently heated by the underlying granite body. The heated fluid then rises back to the surface through fractures and fault-controlled pathways, producing hot spring manifestations.

Fig. 10 illustrates the conceptual model of a radiogenic geothermal system, in which meteoric water penetrates into the subsurface and accumulates in a reservoir located above the granite. The infiltrated water interacts with the granite and is heated by radiogenic heat generated from radioactive decay within the granitic rocks. The heated fluid then migrates upward and emerges at the surface as geothermal manifestations. Fig. 9 presents the 3D model of selected layers (Layer 4 and Layer 8), showing that the granite body (represented in red) intrudes into the overlying formations (represented in yellow). The granite is interpreted to dominate the subsurface lithology beneath the Pemali geothermal area and acts as the primary heat source in the geothermal system.

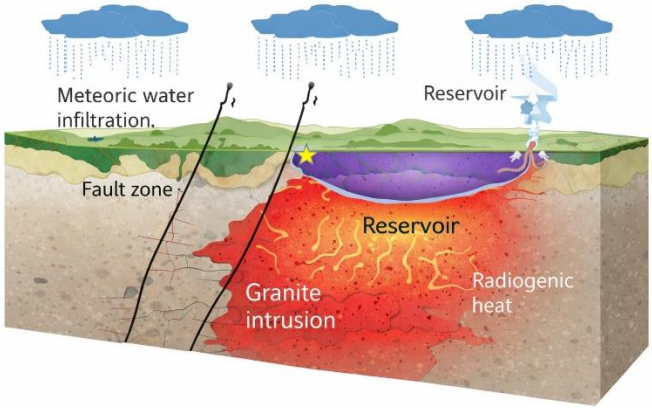

Fig. 10. Radiogenic geothermal system conceptual model in the Pemali geothermal area.

Geologically, Bangka Island is composed of the Pemali Formation/Complex, the Tanjung Genting Formation, alluvial deposits, and granite rocks. The region is dominated by intrusive igneous rocks, where residual heat has decreased over time but the granite bodies still retain significant thermal energy. The presence of granite is interpreted to be associated with radiogenic heat production due to radioactive decay, which may contribute to heat accumulation and is closely related to the occurrence of hot spring manifestations [28, 29].

The geothermal fluid in this system is mainly derived from meteoric water (rainwater) that infiltrates deeply through fault and fracture structures. The meteoric water is interpreted to absorb heat when interacting with the granite body and subsequently forms heated geothermal fluids. These fluids then migrate back to the surface through structurally controlled pathways, producing hot springs as surface geothermal manifestations [16].

5. Conclusion

Based on the gravity data analysis and modeling results, the Complete Bouguer Anomaly (CBA) map indicates that high gravity anomalies dominate most of the study area and are interpreted as Triassic granitic bodies formed from acidic magma intrusion. In contrast, lower anomaly zones observed in the northwestern and northern parts of the Pemali geothermal area are associated with the Tanjung Genting Formation and alluvial deposits, which exhibit relatively lower densities. Spectral analysis and anomaly separation reveal that the regional anomaly represents deep-seated sources with an estimated depth of approximately 4.56 km and positive anomaly values ranging from 21.7 mGal to 38.1 mGal, while the residual anomaly reflects shallower sources at an estimated depth of around 1.68 km, with anomaly values ranging from −2.4 mGal to 1.5 mGal. The low residual anomalies are interpreted as zones influenced by heat transfer from the underlying granite to the overlying sedimentary formations, indicating the presence of a geothermal system.

The 2D and 3D gravity modeling results further suggest that the subsurface structure of the Pemali geothermal area consists of the Pemali Metamorphic Complex as basement rock, granite intrusion, the Tanjung Genting Formation, and alluvial deposits. Fault structures forming a graben system were identified and are interpreted to play a crucial role in controlling the geothermal system. These faults act as conduits for meteoric water infiltration and fluid circulation, allowing water to accumulate within a reservoir zone above the granite body, where it is heated by radiogenic heat generated from the granite. The heated fluids subsequently migrate upward through structurally controlled pathways and emerge as hot spring manifestations at the surface. The relatively moderate temperature range of 40–60°C supports the interpretation of a radiogenic geothermal system rather than a volcanic geothermal system. Overall, the integration of gravity anomaly analysis and subsurface modeling demonstrates that granite intrusion and fault-controlled structures are the primary factors governing the radiogenic geothermal system in the Pemali area.

CRediT authorship contribution statement

Putriani: Writing – review & editing, Writing – original draft, Supervision, Software, Resources, Methodology, Investigation, Formal analysis, Data curation. **Rahmat Nawi Siregar:** Writing – review & editing, Supervision, Resources, Methodology, Investigation, Formal analysis, Data curation, Conceptualization. **Glenaldo Achmad Zhafran Evito:** Writing – review & editing, Investigation.

Declaration of Competing Interest

The authors declare that they have no known competing financial interests or personal relationships that could have appeared to influence the work reported in this paper.

Data availability

Data will be made available on request.

Acknowledgment

The author would like to express sincere gratitude to all individuals and institutions who contributed to the completion of this study. Special thanks are extended to supervisors and academic staff for their guidance, valuable discussions, and continuous support throughout the research process. Appreciation is also given to the institutions that provided geological and geophysical data, as well as to colleagues and collaborators who assisted during data processing, modeling, and interpretation. This research was supported by the facilities that enabled the successful completion of the gravity analysis and geothermal interpretation in the Pemali geothermal area.

References

1. Hosono, T., Hartmann, J., Louvat, P., Amann, T., Washington, K. E., West, A. J., Okamura, K., Böttcher, M. E., and Gaillardet, J. (2018). Earthquake-Induced Structural Deformations Enhance Long-Term Solute Fluxes from Active Volcanic Systems, *Scientific Reports*, Vol. 8, No. 1, 1–12. doi:10.1038/s41598-018-32735-1.

2. Zhang, Z., Yao, H., Wang, W., and Liu, C. (2021). 3-D Crustal Azimuthal Anisotropy Reveals Multi-Stage Deformation Processes of the Sichuan Basin and Its Adjacent Journal of Geophysical Research : Solid Earth, *Journal of Geophysical Research: Solid Earth*, Vol. 127, No. e2021JB023289, 1–17. doi:10.1029/2021JB023289.

3. Liu, S., Suardi, I., Xu, X., Yang, S., and Tong, P. (2021). The Geometry of the Subducted Slab Beneath Sumatra Revealed by Regional and Teleseismic Traveltime Tomography, *Journal of Geophysical Research: Solid Earth*, Vol. 126, No. 1, 1–29. doi:10.1029/2020JB020169.

4. Dewi, K. C. S., Siregar, R. N., Ningati, T. I., Pulungan, Z. N., Indriyawati, A., and Takahashi, H. (2025). Analysis of Subsurface Faults Using 3D Gravity Method Based On Satellite Image Data : Insights into Indo-Australian and Eurasian Plate Subduction in the Formation of An Accretionary Prism, *International Journal of Hydrological and Environmental for Sustainability*, Vol. 4, No. 3, 135–148.

5. Hariyono, E., and S, L. (2018). The Characteristics of Volcanic Eruption in Indonesia, *Volcanoes - Geological and Geophysical Setting, Theoretical Aspects and Numerical Modeling, Applications to Industry and Their Impact on the Human Health*, No. July. doi:10.5772/intechopen.71449.

6. McCaffrey, R. (2009). The Tectonic Framework of the Sumatran Subduction Zone, *Annual Review of Earth and Planetary Sciences*, Vol. 37, 345–366. doi:10.1146/annurev.earth.031208.100212.

7. Hristov, V., Stoyanov, N., Valtchev, S., Kolev, S., and Benderev, A. (2019). Utilization of Low Enthalpy Geothermal Energy in Bulgaria, *IOP Conference Series: Earth and Environmental Science*, Vol. 249, No. 1. doi:10.1088/1755-1315/249/1/012035.

8. Taruna, R. M., and Banyunegoro, V. H. (2018). Earthquake Relocation Using Double Difference Method for 2D Modelling of Subducting Slab and Back Arc Thrust in West Nusa Tenggara, *Jurnal Penelitian Fisika Dan Aplikasinya (JPFA)*, Vol. 8, No. 2, 132. doi:10.26740/jpfa.v8n2.p132-143.

9. Collings, R., Lange, D., Rietbrock, A., Tilmann, F., Natawidjaja, D., Suwargadi, B., Miller, M., and Saul, J. (2012). Structure and Seismogenic Properties of the Mentawai Segment of the Sumatra Subduction Zone Revealed by Local Earthquake Traveltime Tomography, *Journal of Geophysical Research*, Vol. 117, 1–23. doi:10.1029/2011JB008469.

10. Jihad, A., Muksin, U., Syamsidik, and Ramli, M. (2021). Earthquake Relocation to Understand the Megathrust Segments along the Sumatran Subduction Zone, *IOP Conference Series: Earth and Environmental Science*, Vol. 630, 012002. doi:10.1088/1755-1315/630/1/012002.

11. Xu, J., and Kono, Y. (2002). Geometry of Slab, Intraslab Stress Field and Its Tectonic Implication in the Nankai Trough, Japan, *Earth, Planets and Space*, Vol. 54, No. 7, 733–742. doi:10.1186/BF03351726.

12. Kusuhara, F., Kazahaya, K., Morikawa, N., Yasuhara, M., Tanaka, H., Takahashi, M., and Tosaki, Y. (2020). Original Composition and Formation Process of Slab-Derived Deep Brine from Kashio Mineral Spring in Central Japan, *Earth, Planets and Space*, Vol. 72, No. 1. doi:10.1186/s40623-020-01225-y.

13. Malod, J. A., Karta, K., Beslier, M. O., and Zen, M. T. (1995). From Normal to Oblique Subduction: Tectonic Relationships between Java and Sumatra, *Journal of Southeast Asian Earth Sciences*, Vol. 12, Nos. 1–2, 85–93. doi:10.1016/0743-9547(95)00023-2.

14. Li, C. F. (2011). An Integrated Geodynamic Model of the Nankai Subduction Zone and Neighboring Regions from Geophysical Inversion and Modeling, *Journal of Geodynamics*, Vol. 51, No. 1, 64–80. doi:10.1016/j.jog.2010.08.003.

15. Stern, R. J. (2002). Subduction Zones, *Reviews of Geophysics*, Vol. 40, No. 4, 3-1-3–38. doi:10.1029/2001RG000108.

16. Utama, H. W., Mulyasari, R., and Said, Y. M. (2021). Geothermal Potential on Sumatra Fault System To Sustainable Geotourism in West Sumatra, *JGE (Jurnal Geofisika Eksplorasi)*, Vol. 7, No. 2, 126–137. doi:10.23960/jge.v7i2.128.

17. Tabei, T., Hashimoto, M., Miyazaki, S., Hirahara, K., Kimata, F., Matsushima, T., Tanaka, T., Eguchi, Y., Takaya, T., Hoso, Y., Ohya, F., and Kato, T. (2002). Subsurface Structure and Faulting of the Median Tectonic Line, Southwest Japan Inferred from GPS Velocity Field, *Earth, Planets and Space*, Vol. 54, No. 11, 1065–1070. doi:10.1186/BF03353303.

18. Tongkul, F. (2017). Active Tectonics in Sabah – Seismicity and Active Faults, *Bulletin of the Geological Society of Malaysia*, Vol. 64, No. December, 27–36. doi:10.7186/bgsm64201703.

19. Maryanto, S. (2017). Geo Techno Park Potential at Arjuno-Welirang Volcano Hosted Geothermal Area, Batu, East Java, Indonesia (Multi Geophysical Approach), *AIP Conference Proceedings*, Vol. 1908, No. 2017. doi:10.1063/1.5012712.

20. Sujitapan, C., Kendall, J. M., Chambers, J. E., and Yordkayhun, S. (2024). Landslide Assessment through Integrated Geoelectrical and Seismic Methods: A Case Study in Thungsong Site, Southern Thailand, *Heliyon*, Vol. 10, No. 2. doi:10.1016/j.heliyon.2024.e24660.

21. Chambers, J., Holmes, J., Whiteley, J., Boyd, J., Meldrum, P., Wilkinson, P., Kuras, O., Swift, R., Harrison, H., Glendinning, S., Stirling, R., Huntley, D., Slater, N., and Donohue, S. (2022). Long-Term Geoelectrical Monitoring of Landslides in Natural and Engineered Slopes, *Leading Edge*, Vol. 41, No. 11, 768–767. doi:10.1190/tle41110768.1.

22. Whiteley, J. S., Watlet, A., Uhlemann, S., Wilkinson, P., Boyd, J. P., Jordan, C., Kendall, J. M., and Chambers, J. E. (2021). Rapid Characterisation of Landslide Heterogeneity Using Unsupervised Classification of Electrical Resistivity and Seismic Refraction Surveys, *Engineering Geology*, Vol. 290, No. May, 106189. doi:10.1016/j.enggeo.2021.106189.

23. Martinho, E. (2023). *Electrical Resistivity and Induced Polarization Methods for Environmental Investigations: An Overview*, *Water, Air, and Soil Pollution* (Vol. 234), Springer International Publishing. doi:10.1007/s11270-023-06214-x.

24. Kusumayudha, S. B., Lestari, P., and Paripurno, E. T. (2018). Eruption Characteristic of the Sleeping Volcano, Sinabung, North Sumatera, Indonesia, and SMS Gateway for Disaster Early Warning System, *Indonesian Journal of Geography*, Vol. 50, No. 1, 70–77. doi:10.22146/ijg.17574.

25. Meju, M. A., and Le, L. (2002). Geoelectromagneticexploration For Natural Resources:Models, Case Studies and Challenges, *Surveys in Geophysics*, Vol. 23, 133–205.

26. Lange, D., Tilmann, F., Henstock, T., Rietbrock, A., Natawidjaja, D., and Kopp, H. (2018). Structure of the Central Sumatran Subduction Zone Revealed by Local Earthquake Travel-Time Tomography Using an Amphibious Network, *Solid Earth*, Vol. 9, No. 4, 1035–1049. doi:10.5194/se-9-1035-2018.

27. Lin, J. Y., Sibuet, J. C., Hsu, S. K., and Wu, W. N. (2014). Could a Sumatra-like Megathrust Earthquake Occur in the South Ryukyu Subduction Zone?, *Earth, Planets and Space*, Vol. 66, No. 1, 1–8. doi:10.1186/1880-5981-66-49.

28. Siringoringo, L. P., Sapiie, B., Rudyawan, A., and Sucipta, I. G. B. E. (2024). Origin of High Heat Flow in the Back-Arc Basins of Sumatra: An Opportunity for Geothermal Energy Development, *Energy Geoscience*, Vol. 5, No. 3, 100289. doi:10.1016/j.engeos.2024.100289.

29. Hochstein, M. P., and Sudarman, S. (1993). Geothermal Resources of Sumatra, *Geothermics*, Vol. 22, No. 3, 181–200. doi:10.1016/0375-6505(93)90042-L.